American Journal of Pathology, Vol. 156, No. 1, January 2000

Alteration of Pulmonary Neuroendocrine Cells during Epithelial Repair of Naphthalene-Induced Airway Injury

Janice L. Peake,* Susan D. Reynolds,† Barry R. Stripp,† Kimberly E. Stephens,* and Kent E. Pinkerton*

From the Center for Comparative Respiratory Biology and Medicine, University of California, Davis, California; and the Department of Environmental Medicine, School of Medicine and Dentistry,† University of Rochester, Rochester, New York*

Whole-mount airway preparations isolated from the lungs of mice treated by intraperitoneal injection of naphthalene and allowed to recover for 5 days were examined for the distribution and abundance of solitary pulmonary neuroendocrine cells (PNECs) and neuroepithelial bodies (NEBs) along the main axial pathway of the right middle lobe. Sham mice treated with corn oil vehicle were examined in a similar manner. An antibody to calcitonin gene-related peptide, a neuroendocrine cell marker, was used to identify the location, size, and number of PNECs and NEBs in the airways. After naphthalene treatment and epithelial repair, NEBs were significantly increased along the walls of the airways as well as on branch point ridges. The surface area covered by NEBs composed of 20 or fewer PNECs was significantly enlarged after naphthalene treatment compared with control NEBs of an equivalent cell number. The PNEC number per square millimeter was also increased more than threefold above control values after naphthalene treatment. These findings provide further support for a key role of neuroendocrine cells in the reparative process of airway epithelial cell renewal after injury. ***(Am J Pathol 2000, 156:279–286)***

Pulmonary neuroendocrine cells (PNECs) are rare epithelial cells found throughout the bronchial airway tree as solitary cells (PNECs) or clusters of cells (NEBs). These cells secrete a variety of neuropeptides thought to play a role in fetal lung development and airway function.[1–6] PNECs are thought to be increased in chronic lung diseases such as bronchopulmonary dysplasia, cystic fibrosis, and asthma.[7–9] Extended exposure to a variety of pollutants such as tobacco smoke,[10] nitrosamines,[11–13] naphthalene,[14] and ozone[15] or exposure to hypoxic conditions[16] also results in PNEC hyperplasia. The normal physiological functions of PNECs and their neuropeptides in the neonatal and adult lung, as well as in epithelial repair of the airways after injury, are not well understood. It is known that NEBs serve as chemoreceptors that respond to airway hypoxia.[17,18] PNECs and their secretory peptides are also thought to regulate airway tone and pulmonary blood flow during respiration.[1,4–6,19,20] Calcitonin gene-related peptide (CGRP), a known pulmonary vasodilator[6,20] and bronchoconstrictor,[1] is one of several neuropeptides secreted by PNECs.

Owing to the rarity of PNECs and NEBs within the lung airways, mechanisms that lead to hyperplasia of this cell type after epithelial injury are difficult to evaluate. Studies have demonstrated that PNECs contribute less than 0.4% to the total airway epithelium in neonates and less than 0.02% in adults.[21,22] Paraffin sections, even taken from carefully selected tissue blocks of the lungs, are still extremely difficult to use to determine site-specific changes of PNECs in the airways. To overcome this deficiency, a whole-mount immunohistochemical approach was implemented in this study to map the entire axial airway path in one lobe of the lungs.[23] All PNECs in each whole-mount preparation were visualized using CGRP immunoreactivity (CGRP-IR) as a cell marker.

Naphthalene, an aromatic hydrocarbon found in tobacco smoke,[24] destroys nonciliated bronchial epithelial (Clara) cells in the mouse due to activation of cytotoxic epoxides by cytochrome P450–2F2 within these cells.[25] Acute naphthalene toxicity also results in PNEC hyperplasia that is detectable 5 days after treatment.[14] Therefore, we chose to use naphthalene to study the mechanisms of PNEC hyperplasia after epithelial injury, using this same timeframe.

A primary objective of our study was to investigate how PNECs and NEBs respond to acute airway epithelial-cell injury, by addressing the following questions: 1) Is PNEC hyperplasia dependant on airway generation? 2) Do changes in PNECs occur predominantly at airway bifurcations or along airway walls as well? 3) Do the size and shape of NEBs change during the process of epithelial

Supported by National Institutes of Health grants ES01247, ES05707, ES00628, and RR00169 and Tobacco-Related Disease Research Program grants 6RT-0329 and 7RT-0118.

Accepted for publication September 8, 1999.

Address reprint requests to Kent E. Pinkerton, Ph.D., Institute of Toxicology and Environmental Health, One Shields Ave., University of California, Davis, CA 95616. E-mail: kepinkerton@ucdavis.edu.

repair? 4) Do the numbers of PNECs and NEBs change during the period of recovery from naphthalene-induced epithelial injury? Answers to these questions could help us to further understand the location and nature of PNEC hyperplasia in the lungs, because this hyperplasia does not appear to be simply an increase in the size of existing NEBs.[14,26]

Materials and Methods

Animals and Treatment

Animals were obtained from Taconic Farms Animal Breeders (Germantown, NY) and housed in a pathogen-free environment for 1 week of acclimatization and observation before treatment. Naphthalene (300 mg/kg) in corn oil vehicle or vehicle alone was administered intraperitoneally to male FVB/n mice (6 mice/group) at 12 to 14 weeks of age. The lungs were harvested 5 days postinjection and inflation-fixed in 95% ethanol:glacial acetic acid (99:1).

Tissue Preparation and Microdissection

The right middle lobe was used for airway isolation. The main axial airway path was separated from the surrounding parenchyma and vasculature and all airway daughter branches were trimmed off using microsurgical scissors and the aid of a dissecting microscope.[23,27] The axial airway was cut open longitudinally to facilitate subsequent immunohistochemical steps and microscopic observation of the flattened airway under a coverslip. Before immunostaining, the microdissected airways were stored in 70% ethanol.

Reagents

The primary antibody, polyclonal rabbit anti-rat CGRP, was obtained from Sigma Chemical Co. (St. Louis, MO). The biotinylated goat anti-rabbit antibody, goat serum, and avidin-biotin peroxidase complex were purchased from Vector Laboratories (Burlingame, CA). Diaminobenzidine tetrahydrochloride was purchased from Sigma in tablet form. All other fixatives, solvents, and chemicals were purchased from Sigma and Fisher Scientific (Pittsburgh, PA).

Whole-Mount Immunohistochemistry

CGRP, a specific protein marker expressed in neuroendocrine cells, was used to visualize PNECs and NEBs. Immunohistochemistry was performed as previously described,[23] with minor modifications. Briefly, all steps were carried out at room temperature unless otherwise specified. The microdissected airways were dehydrated in ethanol, cleared in xylene, and rehydrated in a graded series of ethanol. Endogenous peroxidase was blocked with aqueous 3% hydrogen peroxide (H_2O_2). Airways were washed in phosphate-buffered saline (PBS) and blocked and permeabilized in 20% goat serum and 0.5% Triton X-100 in PBS for 80 minutes. The airways were incubated for 36–40 hours at 4°C in CGRP antiserum at a dilution of 1:500 in 20% goat serum/PBS-blocking solution. Airways were washed in PBS and incubated in biotinylated goat anti-rabbit antibody at a 1:200 dilution in 20% goat serum/PBS for 4.5 hours at 4°C, followed by 1 hour at room temperature. Airways were washed in PBS and incubated overnight at 4°C in avidin-biotin peroxidase complex reagent made according to Vector Laboratory specifications. The airways were washed in PBS and subsequently immersed in a solution of 0.5% diaminobenzidine tetrahydrochloride, 0.005% NiCl, and 0.075% H_2O_2 for 5 minutes. The reaction was stopped in two changes of PBS. The airways were stored in PBS at 4°C before analysis.

Morphometry

Each airway path was categorized into two distinct anatomical locations: 1) airway bifurcations consisting of the branch point ridge and 2) airway segments or generations forming the region between airway branch points.[23] For ease in identification, airway bifurcations were categorized numerically from a proximal to distal direction beginning at the first intralobar bifurcation of the right middle lobe. This numbering approach was used in place of the more traditional binary classification system,[27] because only the axial pathway was monitored in this study. Airway segments were also numbered beginning with the first airway generation immediately after the first intralobar bifurcation of the right middle lobe (Figure 1).

Airway whole mounts immunostained with CGRP were placed in a pool of PBS on a glass slide, and images were captured with a Leica MZ12 dissecting microscope (Heerbrugg, Switzerland) linked to a Macintosh 2ci computer with a Dage-MTI video camera (Michigan City, IN). All images were captured and analyzed by using the public domain digital image processing software NIH Image (National Institutes of Health, Bethesda, MD). Each whole-mount airway image was traced and used to map and record the location of each CGRP-IR NEB for all airway preparations (Figure 1). NEBs were considered to be two or more adjacent CGRP-IR cells. Cytoplasmic staining of the NEBs with CGRP-IR material was confirmed by embedding the whole-mount airway preparations in Immunobed (Polysciences, Warrington, PA) and cutting 1.5-μm-thick sections (see Figure 8B and Figure 9, A and B, below). Each airway tracing was also used to measure the total surface area from the 1st to the 15th airway generation for each axial airway. Total NEB numbers normalized to surface area could subsequently be expressed for the first 15 airway generations.

Using the map of each airway whole mount as a reference, individual images of each NEB in the airways of all control and naphthalene-treated animals were captured at magnification $\times$40 on an Olympus BH2 light microscope, using a Dage video camera linked to a Macintosh 2ci computer. More than 150 NEBs were imaged for each experimental group along the entire axial airway path.

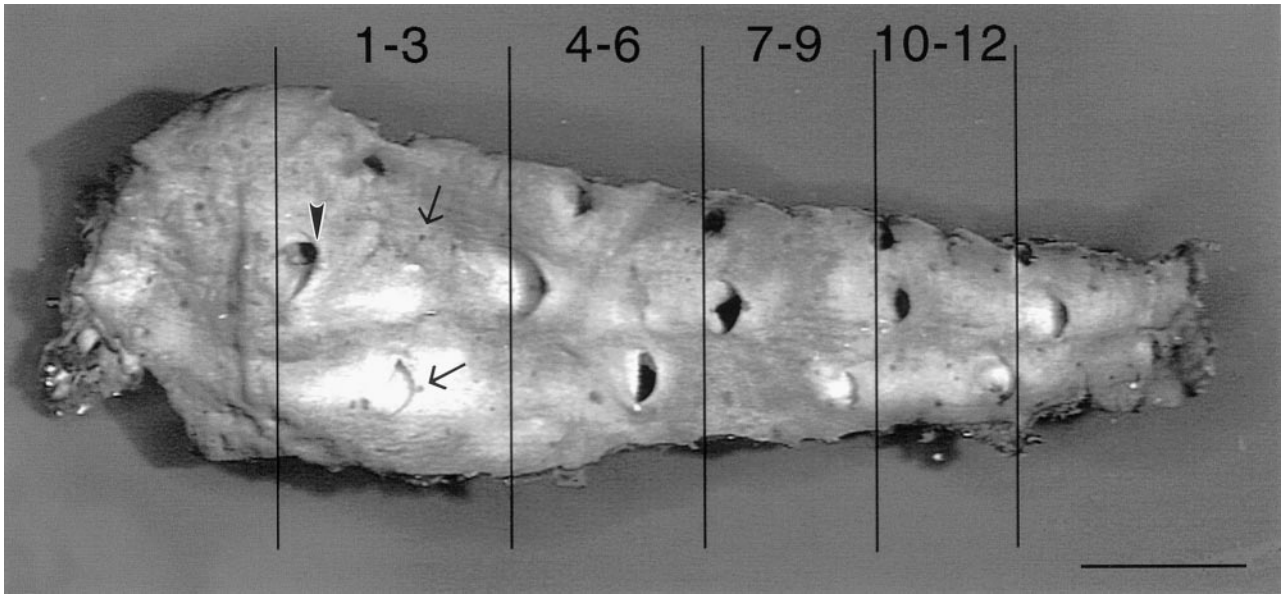

Figure 1. Whole-mount airway preparation of the main axial pathway of the right middle lobe of the mouse. The numerical designation of airway bifurcation ridges begins with the first intralobar bifurcation. The numerical designation of airway generations of the axial pathway also begins immediately after the first intralobar airway branch point (**arrowhead**). Airway generations 1 to 3, 4 to 6, 7 to 9, and 10 to 12 are identified by the **vertical lines** superimposed over the image. NEBs (**arrows**) can be visualized sporadically dotting the surfaces of the airway. Scale bar, 1 mm.

With NIH Image software, the area and shape of each NEB were determined. The numbers of CGRP-IR cells/NEB, as well as the number of nonreactive cells within a NEB, were counted. Solitary PNEC frequency was determined by counting the number of PNECs in four random fields per animal from each airway generation group (ie, airway generations 1–3, 4–6, and 7–9). Each field was photographed with a Dage video camera, using an Olympus BH2 light microscope and a 20× objective lens.

Statistics

All data are presented as mean ± 1 SEM. Five animals were analyzed in the control group, and six animals were analyzed in the group treated with naphthalene. The numbers of NEBs at different airway generations and bifurcation ridges were compared between control and naphthalene groups, using analysis of variance (Statview software v.4.5; Abacus Concepts, Berkeley, CA). The total number of NEBs and the relative density of PNECs between control and naphthalene-treated mice were compared using an unpaired Student's *t*-test. The significance of trends between control mice and mice treated with naphthalene was tested by repeatedly analyzing variances. Significance was considered to be at $P < 0.05$.

Results

PNECs and NEBs along the entire length of the axial airway path of the right middle lobe exhibited CGRP-IR staining. NEBs in control mice were widely scattered along the airway, whereas, in mice treated with naphthalene, NEBs were frequently located in close proximity, in groups of two to three. For both control and naphthalene-treated mice, the total number of CGRP-IR NEBs on bifurcation ridges significantly decreased in a proximal to distal direction along the main axial airway path (Figure 2A; $P < 0.05$). There was also a significant decrease ($P < 0.05$) in the number of CGRP-IR NEBs in proximal airway segments compared with distal airway segments for both control and naphthalene-treated mice (Figure 2B) from airway generations 1 to 15. The reduction in NEB number as a function of branch point number or airway generation was also associated with a decrease in tissue area going from the proximal to distal airways (Figure 1). When the NEB number was normalized to airway surface area (Figure 2C), no significant differences could be detected in NEB numbers from generations 1 to 15 for either control mice or mice treated with naphthalene ($P < 0.05$). NEBs were two- to fivefold more prevalent on airway segments than airway ridges in both control and treated tissue (Figure 2, A and B). Naphthalene treatment was associated with a clear trend of increased numbers of NEBs at both anatomical locations.

To determine whether these trends were significant, the absolute numbers of NEBs present in the first nine bifurcations and airway segments were analyzed. The total number of CGRP-IR NEBs was significantly increased after naphthalene treatment on both bifurcation ridges (Figure 3A) and along airway segments (Figure 3B) compared with the control group ($P < 0.05$). Because absolute numbers of solitary PNECs were difficult to count due to their abundance and small size in the airways, their numbers were expressed per square millimeter of airway surface area, derived from counting a minimum of four randomly selected fields for each group of airway segments. Solitary PNECs were increased threefold after naphthalene treatment compared with control values (Figure 3C; $P < 0.05$).

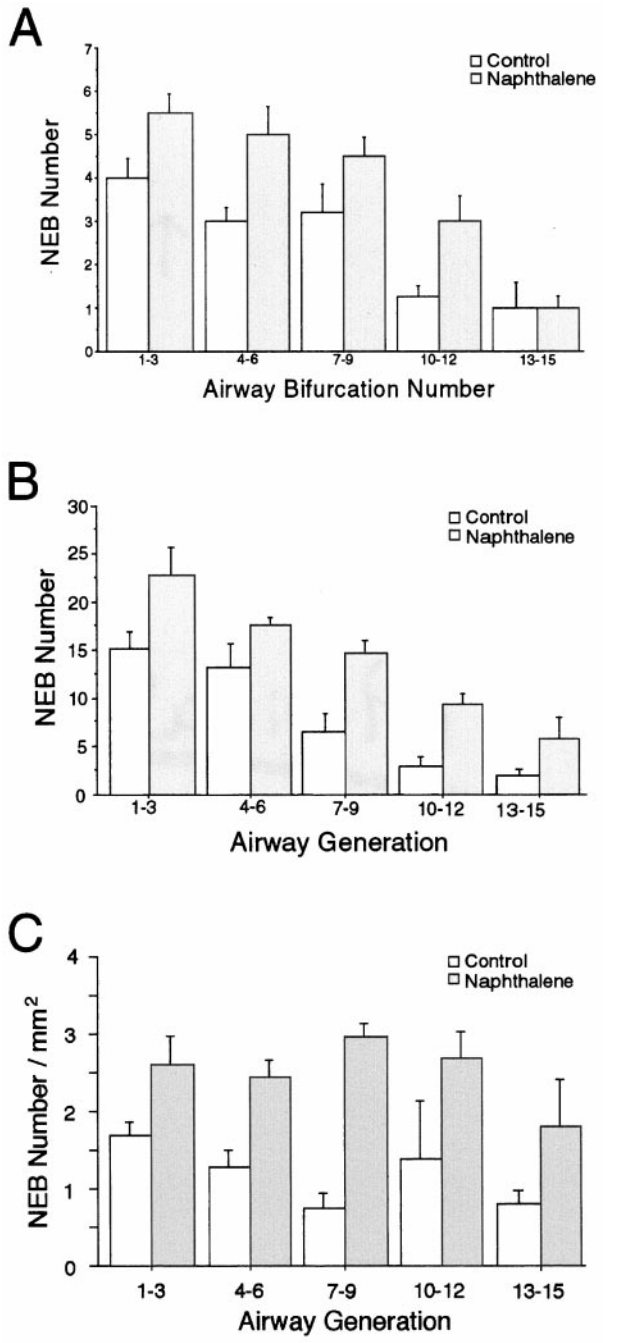

Figure 2. NEB distribution and abundance in the main axial airway path of the right middle lobe in mice treated with corn oil (control) or naphthalene. **A:** The number of NEBs on airway bifurcations; **B:** The number of NEBs on airway generations; **C:** The number of NEBs per square millimeter for different airway generations, demonstrating that NEB frequency was similar along the entire axial airway path.

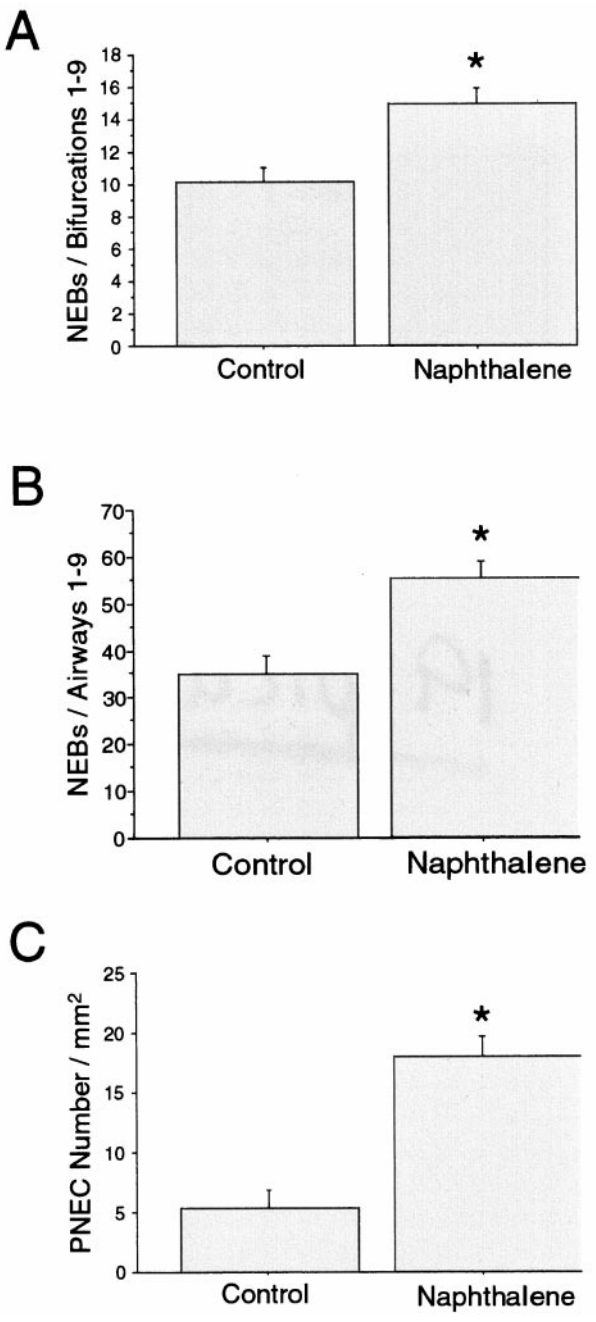

Figure 3. Total NEB numbers found on the first nine bifurcations (**A**) or the first nine airway generations (**B**) of the main axial airway path of the right middle lobe in mice treated with corn oil (control) or naphthalene. The density of solitary neuroendocrine cells (PNECs) is shown (**C**) for control mice and for mice treated with naphthalene. An **asterisk** designates a significant difference from the control value ($P < 0.05$).

The frequency of NEBs grouped by total cell number was analyzed for both control mice and mice treated with naphthalene. NEBs were grouped by total cell number and expressed as a percentage of the total NEB number (Figure 4). Although the proportion of smallest NEBs (ie, cell clusters formed by 2–5 cells) was increased in the airways of mice treated with naphthalene, compared with control mice, this difference was not statistically significant. In contrast, the total surface area of neuroendocrine cell clusters composed of 2 to 5, 6 to 10, 11 to 15, and 16 to 20 cells per NEB was significantly greater in mice treated with naphthalene compared with the control group (Figure 5; $P < 0.05$). Cellular hypertrophy was evident only in NEBs composed of 20 cells or less.

The shape of NEBs observed varied in both control and naphthalene groups. In control mice, the majority of NEBs were compact and uniformly round or ovoid in

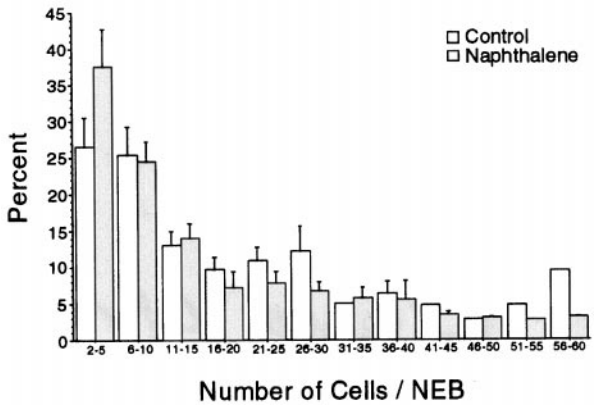

Figure 4. Distribution of NEBs grouped by cell number per NEB for cell clusters of 60 cells or less, expressed as the percentage of the total number of NEBs. The naphthalene mice showed an increase in the smallest NEBs (2–5 cells) compared with control.

shape (Figure 6A). However, approximately 20% were in irregularly arranged shapes (Figure 6B). In mice treated with naphthalene, NEBs also had compact, round shapes similar to those observed in control mice (Figure 6C), but, in contrast, more than 40% of the NEBs had irregular shapes with "budding" cells at the margins of the cell cluster (Figure 6D). These irregularly organized NEBs in the naphthalene-treated group were significantly increased over the control group (Figure 7; $P < 0.05$). NEBs in mice treated with naphthalene frequently appeared to be spreading outward from a central point within the NEB, with unstained cells found in the interior of these bodies and positive cells surrounding them (Figure 8A).

A unique feature of the most irregular NEB formations in mice treated with naphthalene was the presence of small CGRP-IR cells surrounded by more squamated cells (Figure 8, A and B). The shape and size of these neuroendocrine cell clusters were likely to be influenced by the ongoing process of epithelial repair. In tissue sections prepared from airways embedded in immunobed, flattened epithelial cells undergoing re-epithelialization of the airways could clearly be seen surrounding CGRP-IR cells (Figure 9, A and B).

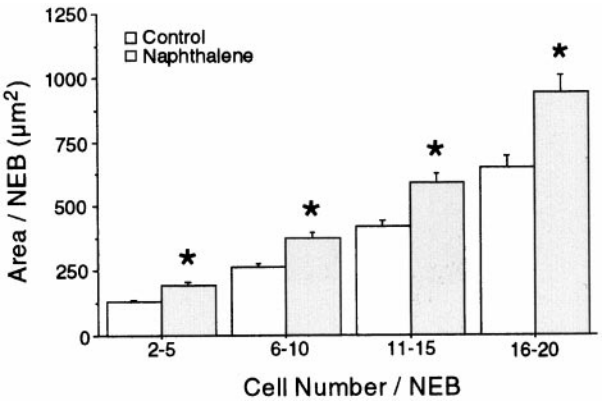

Figure 5. NEB area for cell clusters of different numbers. Treatment of mice with naphthalene was associated with a significant increase in area for NEBs of 20 cells or less in size. An **asterisk** designates a significant difference from the corresponding control value ($P < 0.05$).

Discussion

We have demonstrated that acute airway injury caused by naphthalene injection results in rapid PNEC and NEB hyperplasia and hypertrophy. The repair process of the conducting-airway epithelium is associated with an increase in the number of cells exhibiting CGRP-IR for both solitary PNECs and clusters (NEBs) of neuroendocrine cells. The whole-mount procedure allowed us to sample the entire axial airway path and to document the increase in this rare epithelial-cell population. We were also able to anatomically pinpoint where hyperplasia occurred along the airways. Because the entire NEB could be visualized in each airway segment, we were able to precisely measure the size and shape of each NEB.

Our data demonstrated a significant difference in the number of CGRP-IR NEBs in the proximal airways compared with the distal airways, for both control and naphthalene-treated groups (Figure 2, A and B). However, because total surface area decreases as a function of distance down individual airways, normalization of NEBs to the actual airway surface area present revealed no significant difference in NEB frequency from the proximal to more distal airways of the lungs. Hoyt and colleagues[28,29] found NEBs to be more numerous in proximal airway generations *versus* distal generations. However, this observation was made in a single three-dimensional reconstruction of a hamster lung, using serial paraffin sections. Avadhanam and coworkers[23] also found greater numbers of NEBs in proximal airways *versus* distal airways in whole-mount preparations, but did not normalize NEB frequency to airway surface area.[23] The whole-mount preparation in this study allowed us to sample the entire airway and to normalize the data to the total surface area of the airway. This approach allowed for a more accurate and complete detection of this rare epithelial-cell type than can be done in paraffin sections.

Our data suggest that NEBs along the airway segments, as well as at bifurcation ridges, respond to the same environmental cues. The density of NEBs in both of these regions is constant along the entire proximal-to-distal path of the main axial airway of the right middle lobe (Figure 2C). The relative numbers of NEBs both along airway segments and on airway bifurcations increases in response to naphthalene (Figure 3, A and B). The ratio of segmental NEBs to NEBs within bifurcation zones was constant along the entire airway path (proximal to distal) in both control and naphthalene-treated animals (Figure 2, A and B). Therefore, we conclude that the increase in NEB density after naphthalene exposure is the result of an expansion of both anatomical populations of NEBs.

The increase in NEBs after naphthalene treatment was due in large measure to an increase in small NEBs in the 2- to 5-cell range (Figure 4). This pattern of hyperplasia agrees with the study by Stevens et al,[14] who used an identical mouse injury model injected with naphthalene, as well as that of Joad et al,[26] who used rats exposed to side-stream tobacco. Both groups of investigators reported increased numbers of NEBs, but found that the average size of the NEB was similar in control animals

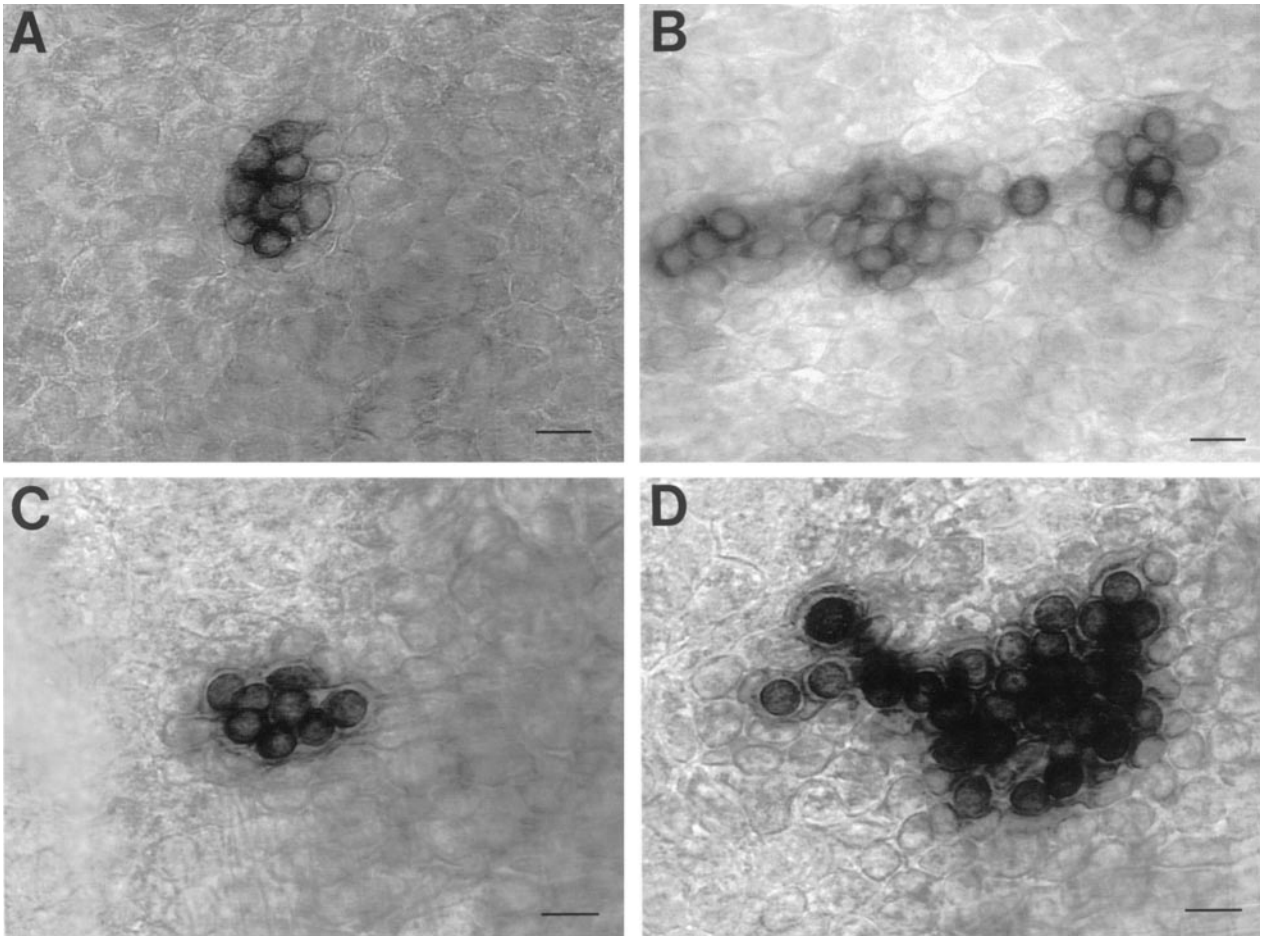

Figure 6. Whole-mount airway images of NEBs in control (**A** and **B**) and naphthalene-treated (**C** and **D**) mice. Compact ovoid clusters of cells were present (**A** and **C**), as well as irregularly arranged clusters of cells (**B** and **D**) in both groups of mice. Scale bar, 20 μm.

compared with treated animals. This finding suggests that the increase in NEBs was due to proliferation of solitary PNECs and small NEBs rather than simply an enlargement of existing NEBs. NEBs containing from 2 to 20 cells/NEB were significantly enlarged based on total surface area per NEB (Figure 5). There was no hypertrophy evident in NEBs larger than 21 cells/NEB. These data correspond well with those of Springall et al,[30] who also reported an increase in CGRP-IR attributed to cell hypertrophy.

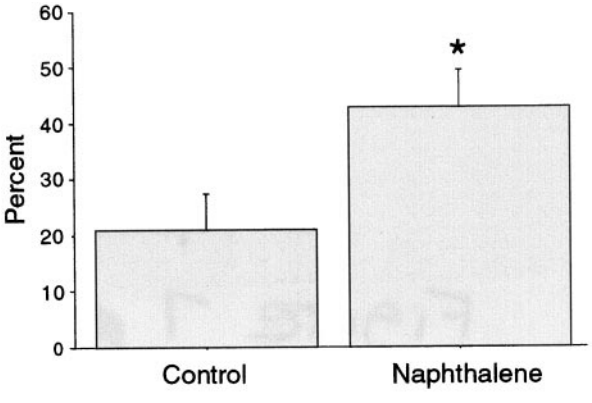

Figure 7. The percentage of irregularly arranged clustered neuroendocrine cells more than doubled in the airways of mice treated with naphthalene compared with control mice. An **asterisk** designates a significant difference from control value ($P < 0.05$).

It should be noted that the unusual shapes (Figures 6 and 8) and close proximity of neighboring NEBs in the airways of animals treated with naphthalene may imply that solitary PNECs "bud off" from larger NEBs, with subsequent proliferation into small NEBs (2–5 cells/body). A number of points support this concept: 1) Cells within large NEBs are more dispersed in the airway epithelium of animals treated with naphthalene (Figure 7), 2) epithelial surfaces undergoing repair contain increased numbers of small NEBs (2–5 cells; Figure 4), 3) NEBs tend to be clustered in the airways of mice after treatment with naphthalene, and 4) epithelial surfaces in the process of repair have an increased number of solitary PNECs (Figure 3C). Hyperplasia of NEBs is likely to involve PNEC proliferation, although we cannot eliminate the possibility that other cells, such as Clara cells, may also differentiate into PNECs.

There was also a significant increase in the number of solitary PNECs within airway generations 1 through 9 (Figure 3C). When averaged for all airway generations, the frequency of these cells increased threefold compared with control. Increases were reported for both

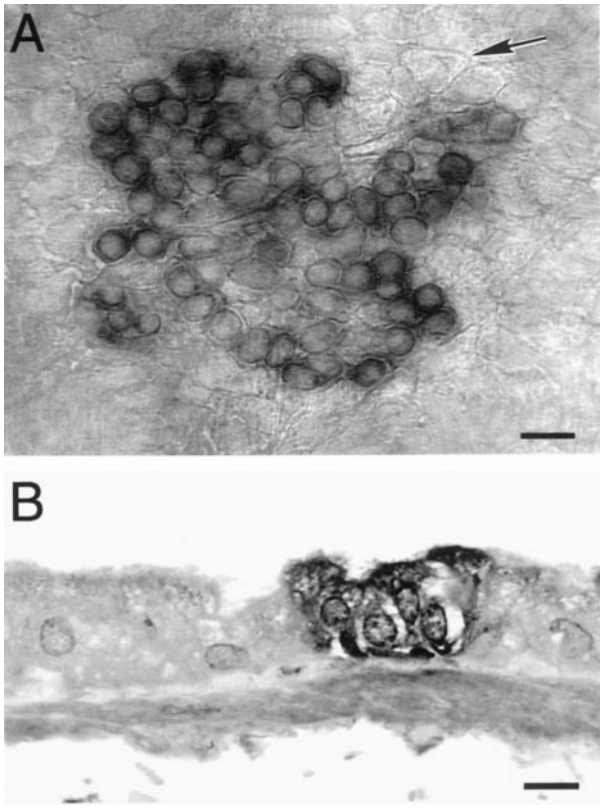

Figure 8. NEB with small CGRP-IR cells intermixed with CGRP-negative bronchiolar epithelial cells of the airway from a naphthalene-treated mouse whole-mount airway preparation. These unstained cells may be PNECs, not expressing this marker, or they could be PNEC precursors. **A:** The NEB appears to be surrounded by larger epithelial cells (**arrow**). In the 1.5-μm-thick plastic section from a whole-mount airway preparation that had been immunostained before embedding and sectioning (**B**), the nuclear density of the NEB is greater than that of the surrounding CGRP-negative epithelial cells. Scale bar, 10 μm.

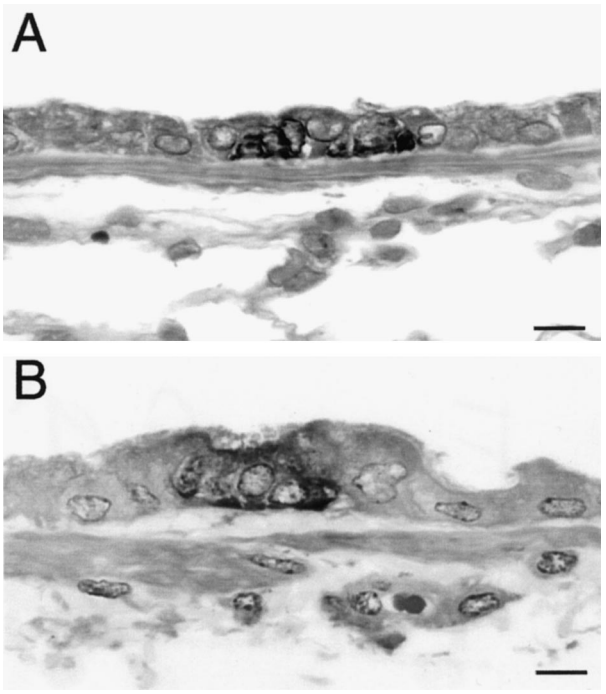

Figure 9. NEBs immunostained as whole-mount airway preparations and subsequently embedded in plastic and sectioned from a control mouse (**A**) and a naphthalene-treated mouse (**B**). The control mouse has an epithelial lining of uniform height and cellularity. In contrast, the mouse treated with naphthalene has an irregular epithelial lining of various heights and cellularity, particularly for those cells in close proximity to the NEB. Scale bar, 10 μm.

PNECs and NEBs in a model of ozone-induced PNEC hyperplasia.[15] This is in contrast to previous work from our laboratory, using paraffin sections,[14] in which hyperplasia was characterized by increased numbers of NEBs; however, a trend toward increased numbers of solitary PNECs did not reach statistical significance, possibly due to insufficient sample size. PNECs are a rare cell type, and the use of the whole-mount preparation allowed us to identify more accurately a statistically significant increase in PNECs throughout all airway generations of the main axial path of the right middle lobe. The number of regions that can be sampled for PNECs was very small in paraffin sections compared with the airway whole mount. In the paraffin sections, less than 0.1 site/mm of basement membrane was found, whereas, in the whole-mount preparation, 5 to 20 solitary PNECs were counted per mm^2 (Figure 3C). The rarity of this cell type requires a large sample area. Because most studies are done on paraffin sections, this may explain why there are conflicting results regarding the hyperplasia of solitary PNECs.

We can only speculate regarding the origin of the additional PNEC at this time. It is possible that the increase in solitary PNECs and small NEBs (five cells or less) in the naphthalene-injured lung is due to proliferation and differentiation of existing PNECs. The irregular shapes of the NEBs in naphthalene-injured lungs suggest that solitary PNECs are derived from existing NEBs. Recent data from our laboratory demonstrate that both Clara cell secretory protein (CCSP)- and CGRP-immunopositive cells within NEBs undergo proliferation based on [^{3}H]-thymidine incorporation.[31] A second possibility is induction of CGRP expression in existing PNECs or PNEC precursors. A third possibility is that solitary PNECs arise from non-pulmonary neuroendocrine progenitor cells and subsequently develop into small NEBs. Other studies suggest that PNEC hyperplasia may be due to proliferation and differentiation of non-CGRP-expressing neuroendocrine cells.[11,13]

We know that Clara cells are injured by naphthalene, but what is the relationship between Clara cell injury and repair and PNEC alterations, including hyperplasia and hypertrophy in the mouse airways? Do PNECs proliferate first to stimulate Clara cell repair? Could they be the progenitor cells for Clara cells, or could they stimulate another cell type to mature into a Clara cell? These are only some of the many interesting questions still to be answered to better understand the role of PNECs in epithelial airway repair after injury.

References

1. Gatto C, Lussky RC, Erickson LW, Berg KJ, Wobken JD, Johnson DE: Calcitonin and CGRP block bombesin- and substance P-induced increases in airway tone. J Appl Physiol 1989, 66:573–577
2. Hoyt RF, Jr, McNelly NA, McDowell EM, Sorokin SP: Neuroepithelial

bodies stimulate proliferation of airway epithelium in fetal hamster lung. Am J Physiol 1991, 260:L234–L240
3. Hoyt RF, Jr, Sorokin SP, McDowell EM, McNelly NA: Neuroepithelial bodies and growth of the airway epithelium in developing hamster lung. Anat Rec 1993, 236:15–22
4. Impicciatore M, Bertaccini G: The bronchoconstrictor action of the tetradecapeptide bombesin in the guinea pig. J Pharm Pharmacol 1973, 25:872–875
5. Lach E, Haddad E, Gies J: Contractile effect of bombesin on guinea pig lung in vitro: involvement of gastrin-releasing peptide-preferring receptors. Am J Physiol 1993, 264(Suppl 8): L80–L86
6. McCormack DG, Salonen RO, Barnes PJ: Effect of sensory neuropeptides on canine bronchial and pulmonary vessels in vitro. Life Sci 1989, 45:2405–2412
7. Aguayo SM: Pulmonary neuroendocrine cells in tobacco-related lung disorders. Anat Rec 1993, 236:122–127
8. Gosney JR, Sissons MC, Allibone RO, Blakey AF: Pulmonary endocrine cells in chronic bronchitis and emphysema. J Pathol 1989, 157:127–133
9. Johnson DE, Anderson WR, Burke BA: Pulmonary neuroendocrine cells in pediatric lung disease: alterations in airway structure in infants with bronchopulmonary dysplasia. Anat Rec 1993, 236:115–119
10. Sunday ME, Kaplan LM, Motoyama E, Chin WW: Biology of disease: gastrin-releasing peptide (mammalian bombesin) gene expression in health and disease. Lab Invest 1988, 59:5–24
11. Linnoila RI: Effects of diethylnitrosamine on lung neuroendocrine cells. Exp Lung Res 1982, 3:225–236
12. Sunday ME, Willet CG: Induction and spontaneous regression of intense pulmonary neuroendocrine cell differentiation in a model of preneoplastic lung injury. Cancer Res Suppl 1992, 52:S2677–S2686
13. Sunday ME, Willet CG, Patidar K, Graham SA: Modulation of oncogene and tumor suppressor gene expression in a hamster model of chronic lung injury with varying degrees of pulmonary neuroendocrine cell hyperplasia. Lab Invest 1994, 70:875–888
14. Stevens TP, McBride JT, Peake JL, Pinkerton KE, Stripp BR: Cell proliferation contributes to PNEC hyperplasia after acute airway injury. Am J Physiol 1997, 272(Suppl. 16):L486–L493
15. Ito T, Ikemi Y, Ohmori K, Kitamura H, Kanisawa H: Airway epithelial cell changes in rats exposed to 0.25 ppm ozone for 20 months. Exp Toxicol Pathol 1994, 46:1–6
16. Keith IM, Will JA: Dynamics of the neuroendocrine cell-regulatory peptide system in the lung (specific overview and new results). Exp Lung Res 1982, 3:387–402
17. Lauweryns JM, Cokelaere M, Lerut T: Cross circulation studies on the influence of hypoxia and hypoxemia on neuro-epithelial bodies in young rabbits. Cell Tissue Res 1978, 193:373–386
18. Youngson C, Nurse C, Yeger H, Cutz E: Oxygen sensing in airway chemoreceptors. Nature 1993, 365:153–155
19. Salonen RO, Webber SE, Widdicombe JG: Effects of neuropeptides and capsaicin on the canine vasculature in vivo. Br J Pharmacol 1988, 95:1262–1270
20. Tjen-A-Looi S, Ekman R, Lippton H, Cary J, Keith I: CGRP and somatostatin modulate chronic hypoxic pulmonary hypertension. Am J Physiol 263(Suppl. 32):H681–H690
21. Gillan JE, Pape KE, Cutz E: Association of changes in bombesin immunoreactive neuroendocrine cells in lungs of newborn infants with persistent fetal circulation and brainstem damage due to birth asphyxia. Pediatr Res 1986, 20:828–833
22. Gosney JR, Sissons MC, Allibone RO: Neuroendocrine cell populations in normal human lungs: a quantitative study. Thorax 1988, 43:878–882
23. Avadhanam KP, Plopper CG, Pinkerton KE: Mapping the distribution of neuroepithelial bodies of the rat lung: a whole-mount immunohistochemical approach. Am J Pathol 1997, 150:851–859
24. Schmeltz I, Tosk J, Hoffman D: Formation and determination of naphthalenes in cigarette smoke. Anal Chem 1976, 48:645–650
25. Plopper CG, Macklin J, Nishio SJ, Hyde DM, Buckpitt AR: Relationship of cytochrome P-450 activity to Clara cell cytotoxicity. III. Morphometric comparison of changes in the epithelial populations of terminal and lobar bronchi in mice, hamsters and rats after parenteral administration of naphthalene. Lab Invest 1992, 67:553–565
26. Joad JP, Ji C, Kott KS, Bric JM, Pinkerton KP: In utero and postnatal effects of sidestream cigarette smoke exposure on lung function, hyperresponsiveness, and neuroendocrine cells in rats. Toxicol Appl Pharmacol 1995, 132:63–71
27. Plopper CG: Structural methods for studying bronchiolar epithelial cells. Models of Lung Disease: Microscopy and Structural Methods. Edited by J Gil. New York, Marcel Dekker, 1990, pp 537–559
28. Hoyt RF, Jr, Sorokin SP, Feldman H: Small-granule (neuro)endocrine cells in the infracardiac lobe of a hamster lung: number, subtypes, and distribution. Exp Lung Res 1982, 3:273–298
29. Hoyt RF, Jr, Feldman H, Sorokin SP: Neuroepithelial bodies (NEB) and solitary endocrine cells in the hamster lung. Exp Lung Res 1982, 3:299–311
30. Springall DR, Collina G, Barer G, Suggett AJ, Bee D, Polak JM: Increased intracellular levels of calcitonin-gene related peptide-like immunoreactivity in pulmonary endocrine cells of hypoxic rats. J Pathol 1988, 155:259–267
31. Reynolds SD, Giangreco A, Power JHT, Stripp BR: Neuroepithelial bodies of pulmonary airways serve as a reservoir of progenitor cells, capable of epithelial regeneration. Am J Pathol 2000, 156:269–278